AEROACOUSTIC AND AERODYNMAMIC PERFORMANCE OF SILENCER UNITS AT DIFFERENT INFLOW PROFILES

Johannes WALTER, Johannes RAU, Martin GABI

Fachgebiet Strömungsmaschinen, Kaisertraße 12, 76131 Karlsruhe, Germany

SUMMARY

Silencer units are installed downstream of axial fans to reduce the noise emission. An inhomogeneous or swirling fan outflow profile, respectively inflow profile to the silencer unit, leads to increased aerodynamic losses. Additionally, the acoustic properties are impaired by the sound generation of areas with high flow velocity. Experiments are carried out on a scaled test rig, which is based on a state of the art configuration. Total and static pressure measurements are conducted in the diffuser, the silencer and downstream the silencer. The results show that there is a strong dependence of the performance of the configuration on the diffuser inlet profile. The undisturbed or hubstrong inflow profile leads to the formation of a high velocity area in the center of the splitter silencer. The tipstrong inlet and swirl inflow profiles lead to the opposite behavior. There are high velocities close to the casing and low or negative velocities in the center. The loss coefficient of the silencer unit can increase up to 170 % depending on the inflow profile. The flow noise, which is generated at the outlet of the splitters, is investigated as well. Therefore two characteristic silencer flow profiles are reproduced. Additionally, a nearly homogeneous flow distribution in the silencer is investigated as a reference. The results show that the flow noise for the characteristic silencer flow profiles is up to 11 dB higher than for the reference flow profile. The spectra K are in good agreement with the results of Kårekull et al. [1].

INTRODUCTION

Dissipative splitter silencers are used to reduce the noise emission in conventional HVAC systems as well as in process industry and thermal power stations. One of the main sources for noise emission in ventilation systems is the fan [2]. A typical configuration consists of the fan, the duct section and the splitter silencer. The duct section can be divided in two parts, the diffuser of the fan DF and a duct transition DT. This DT connects the circular diffuser outlet to the rectangle cross-section of the silencer and compensates the blockage of the splitters. A schematic view of a fan-silencer configuration is shown in figure 1. The fan outflow profile depends on the fan design and on the operation point. It is distinguished between fans with and without outlet guide vanes. The installation of outlet guide vanes leads to a conversion of the swirl into a further pressure rise. The free vortex design of the impeller

has been very common in the past and still today. For this design type the outflow profile is uniform, considering an inviscid flow with isoenergetic and axially parallel inflow to the fan [3].

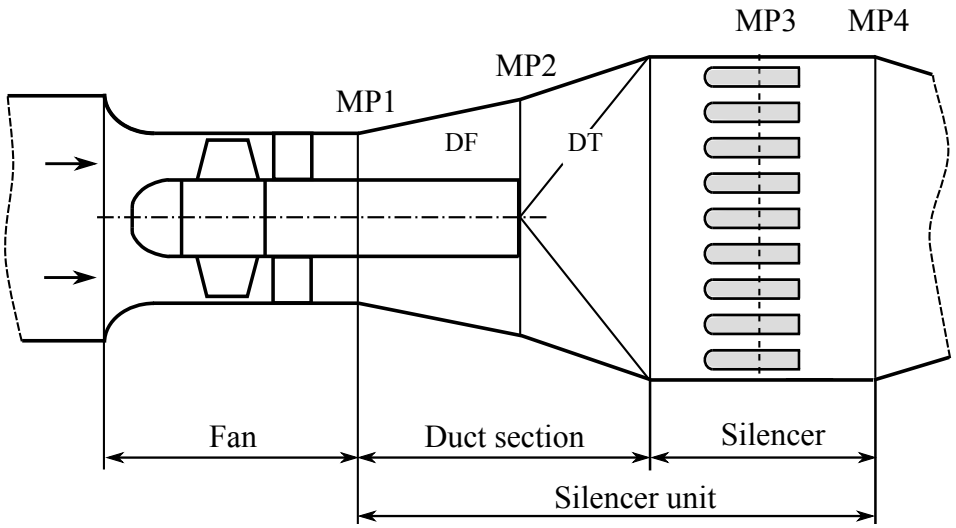

Figure 1: Configuration

Other vortex design criteria or an off design operation of the fan can cause disturbed outflow profiles. The profiles are divided in three characteristic types: an undisturbed inflow profile HOM (Fig. 2, left), a hubstrong profile HS (Fig. 2, center) and a tipstrong profile TS (Fig. 2,right).

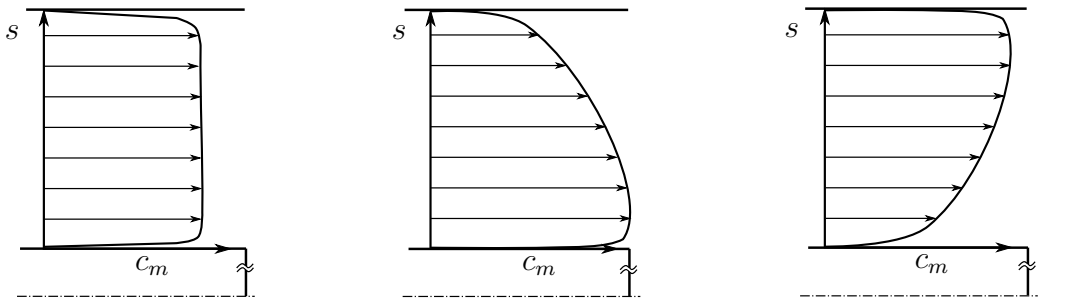

Figure 2: Fan outflow profiles

The outflow profile of the fan can trigger flow separation in the diffuser DF or the duct transition DT. This leads to a non-uniform flow in the silencer with local high and low velocity areas. The interaction of the components is often neglected in the design stage of a silencer unit. One the one hand this often causes higher losses than in the design stage estimated. On the other hand the acoustic properties of the unit may be impaired due to flow noise. According to [4] the attenuation of a silencer should only be determined without flow up to a maximum velocity of $20\,m/s$. For higher velocities the flow noise and the influence of the flow on the attenuation must be considered.

In the first part it is shown that a non-uniform or swirl impaired outflow profile of the fan can have a strong impact on the diffuser and silencer flow and thus on the losses. These results are based on the publication of the author at [5]. In the second part the flow noise is studied. The silencer flow profiles are reconstructed with the results of the first part. The acoustic design of the silencer is not addressed. The interested reader may refer [6], [7].

AERODYNAMIC PROPERTIES

Experimental setup

Investigations are conducted at a scaled test rig. Therefore typical fan outflow profiles are reconstructed and used as inflow to the model of the silencer unit. The geometry is based on a state of the art configuration with the hub to tip ratio ν at the inlet to the test section of 0.5 with the annular gap height S. A schematic view of the test rig is shown in figure 3. The diffuser DF is designed according to the design chart of Sovran and Klomp [8] with an opening angle of $2\alpha_{DF} = 14.6°$ and a length of $4.7S$. Since the DT changes the cross section, the opening angle α_{eff} of a conical diffuser with identical length ($4.8S$) and area ratio is considered. The effective angle of the DT is $\alpha_{eff,DT} = 34°$ and therefore very high. However, an optimized design according to the design chart of [8] would lead to an approximately three times higher length. Therefore this short design corresponds to the state of the art because of the lower demand for installation space. The splitters of the silencer have semicircular leading edges to reduce the inflow losses. They are positioned in the rectangular cross section of the silencer $5.3S$ downstream the hub. The width of a splitter body and the channel between two splitters is $2h$, the width of the wall near channels is h. Consequently, the blocked area due to the installation of the silencer is 50 % of the cross section. Upstream and downstream the test object are chambers. Chamber one is equipped with screens and a flow straightener. The volume flow is generated by a centrifugal fan which is connected to chamber two (reverberation room). Silencers SI are installed to reduce the noise of the fan. Three measurement planes are introduced: MP1 at inlet to the silencer unit, MP2 in the cross section between the splitters and MP3 the outlet. (Fig. 1).

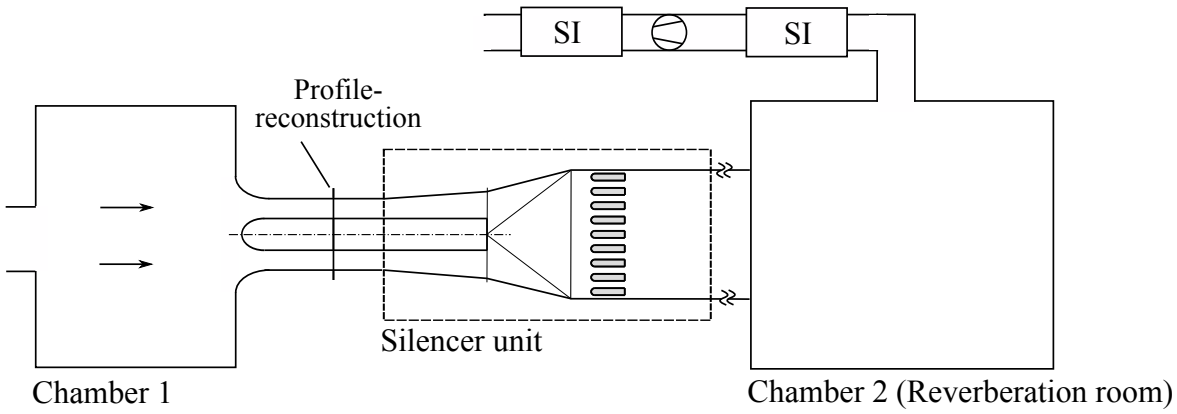

Figure 3: Schematic view of the test rig

In order to determine the loss coefficient ζ of the silencer unit, grid measurements with pressure probes are conducted at the inlet and outlet of the unit. The loss coefficient is mass flow averaged.

$$\zeta = \frac{p_{tot,1} - p_{tot,3}}{p_{dyn,1}} \tag{1}$$

(2)

The measurement error strongly depends on the resolution of the measurement grid. To quantify this, reference measurements with a calibrated volume flow measurement-nozzle are continuously carried out. The volume flow, which is determined by the grid measurements, is compared to the volume flow at the nozzle. The deviation at the inlet (MP1) is smaller than 3 % for all inflow profiles. The error in MP3 is higher (max. 8 %) due to the strongly inhomogeneous outflow.

Furthermore, the blocked-area fraction B (eq. 3) of the silencer flow is analyzed to determine the

homogeneity of the profile.

$$B = 1 - \frac{1}{A} \int_A \frac{c_{ax}}{c_{ax,max}} dA \tag{3}$$

A is the flow area in the corresponding cross section. Flow resistance sheets or a swirl generator are installed upstream the silencer unit to generate the desired inlet profiles. The installation of these sheets leads to a reproduction of the tipstrong profile TS respectively the hubstrong profile HS. The geometry of the sheets is described in [9]. Furthermore, three swirling inflow profiles are generated. The flow angles α are constant over the annular gap height. This is chosen to allow a systematic analyzation of the resulting losses. The three inflow profiles $SW20, SW30, SW40$ with the corresponding swirl angles of $20°, 30°, 40°$ are studied. The profiles are displayed in figure 4 over the annular gap height S. The velocities are related to the area-averaged mean velocity in the inlet section.

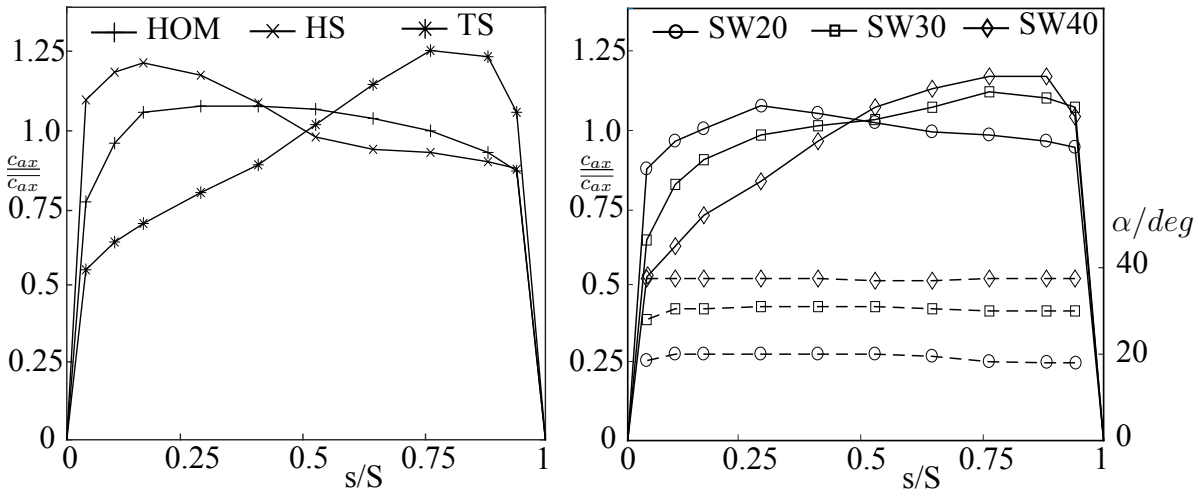

Figure 4: Inflow profiles to the silencer unit

The maximum velocity $c_{ax,max}$, the corresponding annular gap position $s_{c_{ax,max}}$ and the blocked area fraction B are given in table 1 for the inlet profiles.

Table 1: Inflow characteristics

Profile	HOM	HS	TS	$SW20$	$SW30$	$SW40$
$c_{ax,max,1}/\overline{c_1}$	1.07	1.21	1.26	1.07	1.10	1.18
$s_{c_{ax,max,1}}/S$	0.29	0.17	0.78	0.28	0.76	0.78
B_1	0.08	0.19	0.21	0.08	0.09	0.18

Results

The flow distributions in the splitter silencer are analyzed. The profiles are related to the area averaged velocity and displayed as contour plots. The loss coefficient ζ is related to a reference value. Therefore the loss coefficients of the single components are taken from literature ([8], [10], [11]) and added in consideration of the area ratios. This results in the reference loss coefficient ζ_{Ref} of 0.23.

The flow profiles in the silencer (MP3) can be categorized in two groups. The undisturbed and hubstrong inflow profiles (HOM, HS) lead to high velocities in the center of the silencer, while in the

outer region no flow or small velocities are measured. In contrast, the tipstrong and swirling inflow (TS, $SW20$, $SW30$, $SW40$) cause high velocities close to the casing of the silencer. The wake area downstream the hub is still present in the center of the silencer.

The inflow profile HOM, as a representative of the first group, is discussed. The velocity distribution is shown in figure 5 on the left. The contour plot of the velocity in the silencer is determined with measurement results at the positions x, the boundary layers are neglected. The maximum velocities $c_{max,3}$ occur in the center with $2.09\,\overline{c}_3$. This characteristic flow profile can be lead back to the high opening angle of the duct transition DT. The flow cannot follow the contour and separates at the casing. There are high velocities in MP2 at a circular region with the dimension of the outlet of diffuser DF $A_{3.1}$. 78 % of the volume flow pass the silencer through this area $A_{3.1}$. The losses are 30% higher than the reference value. The hubstrong inflow HS shows similar characteristics, the parameters are summed up in table 2.

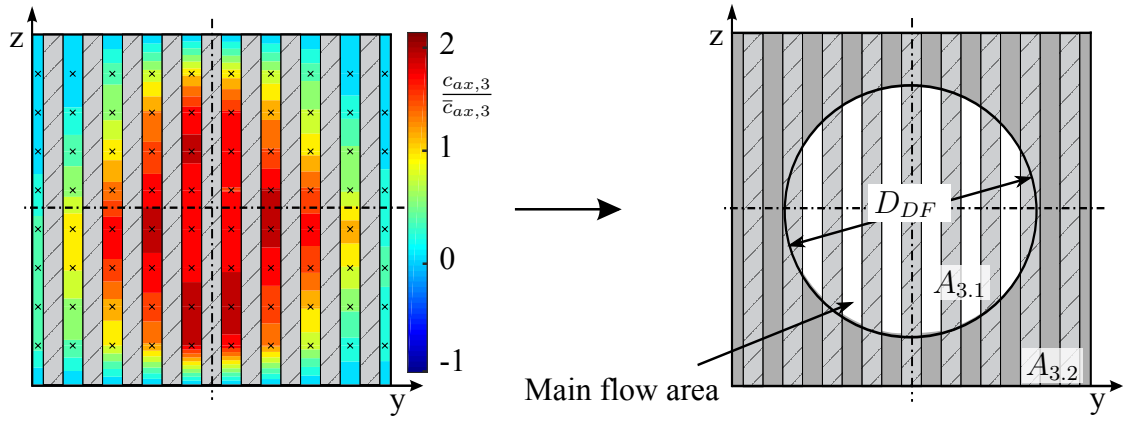

Figure 5: Left: Flow distribution between the silencer splitters for profile HOM, right: Projection of diffuser outlet area on the silencer

The tipstrong inlet profile represents group two. The flow cannot follow the contour of the hub and causes an extended wake area downstream the hub which is still existent in the splitter silencer (Fig. 6, left). This leads to high velocities in the outer area of the silencer, while in the center no forward flow is detected. In order to analyze the volume flow distribution the reference area $A_{3.2}$ (Fig. 6, right) is introduced analogous to the first profile group. 77 % of the volume flow pass this area. The maximum velocity is $c_{ax,max,3} \approx 1.93\,\overline{c}_{ax,3}$. The inlet profile $T2$ leads to an increase of the loss coefficient of 86 % compared to the reference value.

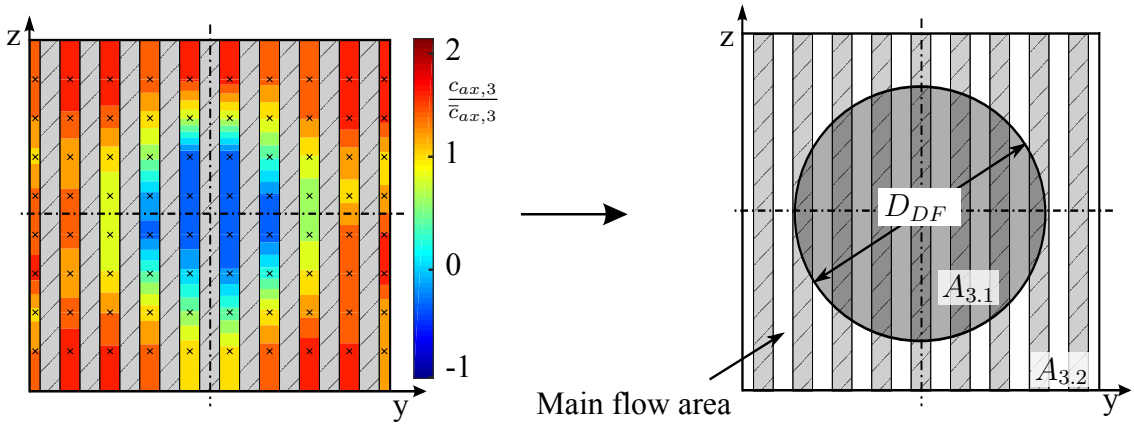

Figure 6: Left: Flow distribution between the silencer splitters for profile TS, right: Projection of diffuser outlet area on the silencer

A swirling inflow to the silencer unit leads to a similar flow characteristic. The flow incidence at the leading edges of the silencer causes additional losses, therefore the loss coefficient ζ increases up to $2.69\ \zeta_{Ref}$ for $SW40$.

The results are in good agreement with the findings of Ackermann [11]. He figured out, that the loss coefficient ζ of the splitter silencer can significantly increase compared to an undisturbed inflow.

Table 2: Silencer flow characteristics

Profile	HOM	HS	TS	$SW20$	$SW30$	$SW40$
ζ/ζ_{REF}	1.30	1.48	1.69	1.44	1.95	2.69
$c_{ax,max,3}/\overline{c}_{ax,3}$	2.09	1.84	1.93	2.21	2.73	3.45
$\dot{V}_{3.1}/\dot{V}$	0.78	0.70	0.25	0.23	0.14	0.01
$\dot{V}_{3.2}/\dot{V}$	0.22	0.30	0.75	0.77	0.86	0.99
B_3	0.08	0.19	0.21	0.08	0.09	0.18

AEROACOUSTIC PROPERTIES

The main noise source of the splitter silencer is the radiation area at the splitter outlet. This source has a dipole character and its strength depends on the flow velocity. The noise generated by turbulence is of minor significance. The resulting noise should be at least 5 dB below the target sound power level downstream the silencer, otherwise the acoustic properties are impaired [6]. In the design stage of a silencer unit, the cross section A_3 is often determined with the desired volume flow and the critical velocity (assuming a uniform profile) in the silencer. However, in real silencer units the flow distribution is often not uniform and this causes local high and low velocity areas as shown in the section before.

Nelson and Morfey [12] developed a scaling law for noise generation in low speed flow ducts by using a generalized spectrum. The effect of turbulence is neglected by the assumption of a homogeneous flow. Their model is based on the dipole characteristics of the noise source and the assumption that the rms value of the fluctuating drag force F is proportional to the mean drag force F. They determine the force F with the static pressure drop Δp over the duct constriction and the open area ratio σ. Oldham and Ukpoho [13] introduced a more general formulation by using the dependence of the area ratio from the pressure drop. In a more recent publication Kårekull et. all used a momentum flux based scaling [14]. This model shows a better accuracy for duct constrictions with high pressure loss.

Scaling law for flow noise

According to [1] the acoustic power W_D of the source in a frequency band is defined as the product of radiation resistance R and the force auto-spectrum S_{FF} which is a function of the Strouhal number .

$$W_D = R_{rad} S_{FF}(St) \tag{4}$$

Nelson und Morfey [12] relate the auto-spectrum of the force S_{FF} to the mean drag force $\overline{F}$ (Gl. 5).

$$S_{FF} = K^2(St)\,\overline{F}^2 \tag{5}$$

This means the generalized spectrum K is a function of the Strouhal number St and thus allows the scaling of the acoustic power. The equations 4 and 5 lead to:

$$K^2(St) = \frac{W_D}{R_{rad}\,\overline{F}^2}. \tag{6}$$

In order to determine the generalized spectrum K the Strouhal number has to be defined. Furthermore the acoustic power W_D with corresponding force F and the radiation resistance R_{rad} is needed. The radiation resistance R_{rad} is only a function of the channel geometry below the cut-off frequency. Above $f_{cut,off}$ there is also a dependence on the frequency f, since higher modes can propagate. R_{rad} is defined according to [1]:

$$f < f_{cutoff} \quad R_{rad} = \frac{1}{4A\rho_0 a_0} \tag{7}$$

$$f > f_{cutoff} \quad R_{rad} = \frac{\pi f^2}{6\rho_0 a_0^3}\left(1 + \frac{3a_0}{8f}\cdot\frac{L_2 + L_3}{A}\right). \tag{8}$$

L_2 and L_3 are the lateral dimensions of the channel, A is the cross section. For the determination of the Strouhal number St (eq. 10) characteristic dimensions have to be defined. The hydraulic diameter d_{hyd} (eq. 9) of the silencer is used as reference. A_3 is the cross section of the non-blocked area between the splitter bodies and the corresponding velocity c_3.

$$d_{hyd} = \sqrt{\frac{4\,A_3}{\pi}} \tag{9}$$

$$St = \frac{f\,d_{hyd}}{c_3} \tag{10}$$

The steady force $\overline{F}$ is defined according to [14] with the momentum flux at the outlet between the absorber bodies.

$$\overline{F} = \dot{m}\cdot c_3 \tag{11}$$

Experimental setup

The sound power measurements are carried out in accordance with ISO 7235 [4]. The results are determined in third octave bands from 200 Hz to 16000 Hz. The volume V of the reverberation chamber is $99\,m^3$.

The test setup has to be modified for this investigation. The installations upstream the silencer (resistance sheets, hub, diffuser) lead to noise. The desired minimum distance of 10 dB [4] to the flow noise at the area of interest (absorber outlet) and background noise was not obtained. Therefore the test object is placed at the entrance to the reverberation room and the installations upstream the test object are removed (Fig. 7). Additionally, the silencers SI are installed. This way the minimum distance of approximately 10 dB to the noise upstream the test object over the frequency band of interest is achieved. The sound power in this setup is radiated directly into the reverberation room. Since the dimensions of the reverberation room $L_2 + L_3$ are small compared to its cross section A, the radiation resistance will approach

$$f > f_{cutoff} \quad R_{rad} = \frac{\pi f^2}{6\rho_0 a_0^3}. \tag{12}$$

All frequencies of interest are above the cut off frequency f_{cutoff}.

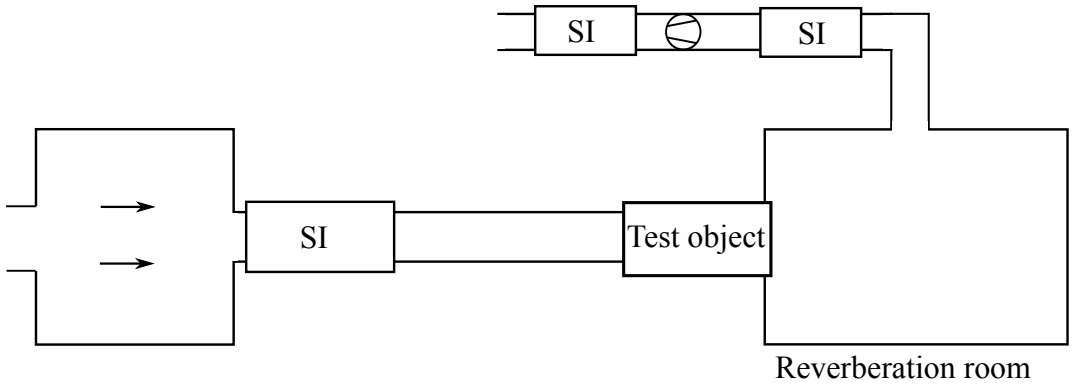

Figure 7: Sketch of measurement setup

However, due to this modification a new concept for the reconstruction of the silencer flow profiles has to be introduced. Therefore the characteristic flow areas of the two groups are considered (Fig. 5, 6). The cross sections $A_{3.1}$ receptively $A_{3.1}$ are blocked to reproduce the profile characteristics. The new silencer profiles are named HOM^* and TS^*. Additionally, a reference configuration REF is investigated with an undisturbed, nearly homogenous silencer flow. The test objects are shown in figure 8. σ is the area ratio of the channel cross section A to the non-blocked area between the absorber A_3^*. For the reference profile σ equals 0.5 and for the profiles HOM^* and TS^* 0.23 respectively 0.27.

The velocity profiles in the silencer are analyzed analogously to the section before. The maximum deviation of the velocity is for all profiles smaller than 9 % at the measurement locations. The resulting profiles approach the characteristics of the profiles in the aerodynamic study.

The mean velocity in the non-blocked flow area of profile HOM^* is $\overline{c}_{ax,3,HOM^*} = 2.17\,\overline{c}_{ax,3,REF}$ and corresponds approximately to the maximum velocity of configuration HOM. The mean velocity of profile TS^* is $\overline{c}_{ax,3,HOM^*} = 1.85\overline{c}_{ax,3,REF}$ and therefore close to the maximum velocity for configuration TS^*.

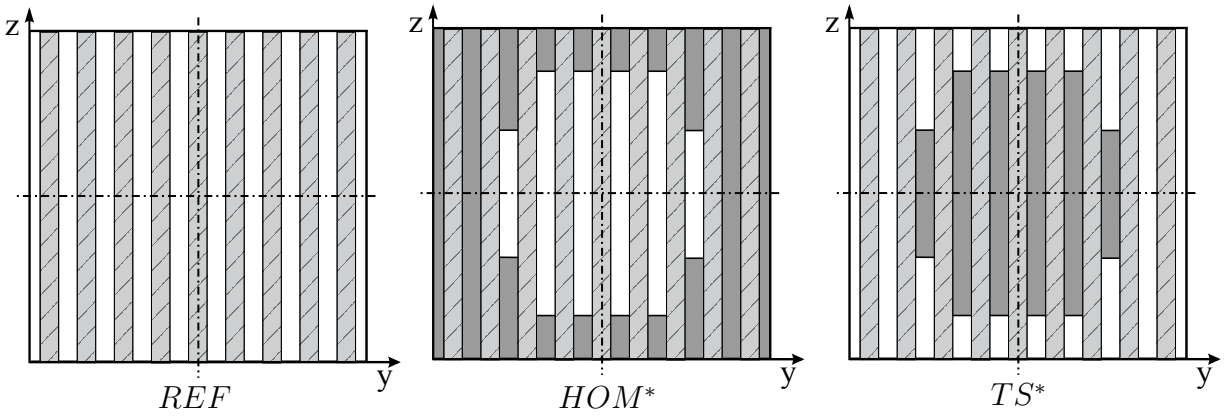

Figure 8: Test objects

The measurements of the flow noise are carried out for different velocities. The minimum velocity is limited, as mentioned, by the required distance to the background noise of 10 dB. This is achieved for a flow velocity c_3 at the absorber outlet of at least $26\,m/s$. This is higher than the critical velocity of 20 m/s [4]. In order to evaluate the noise generation at 20 m/s the results are scaled.

Results

The generalized spectrum K is plotted in figure 9 as $10\log(K^2/10^{-12})$ over the Strouhal number St. The profiles REF, HOM^*, TS^* are marked with the symbols $\times$, $\triangleleft$, $\circ$. The channel velocities c are represented in different colors. For $St > 10$ all measurements lead to similar results. At smaller Strouhal numbers ($St < 10$) the dispersion of the results is higher. This might be influenced by the characteristic vortex shedding frequencies. However, considering the generalized spectrum of the single profiles for different velocities, the results show the same characteristics over the complete frequency band.

Kårekull et al. [1] conducted experiments on flow duct constriction noise for different components. They found the universal trend of

$$K(St) = 68 - 28\log(St) \quad St > 3. \tag{13}$$

This is in good agreement with this investigation, especially for $St > 10$. The peaks due to the characteristic vortex shedding frequencies are present at smaller Strouhal numbers.

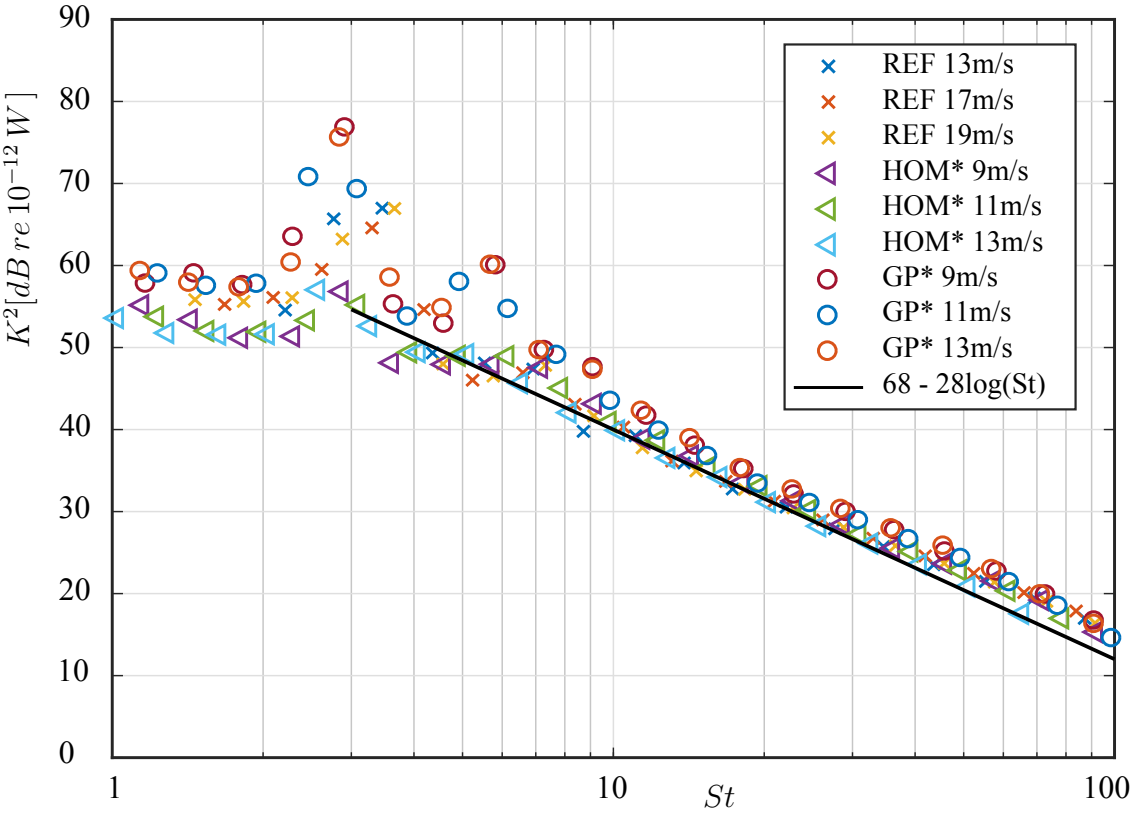

Figure 9: Generalized spectrum K

Based on these results, the sound power level at a channel velocity c of 10 m/s, respectively 20 m/s between the splitters without additional blockage is determined. The results are shown in figure 10. On the left the sound power level SPL is plotted over the frequency f. The benefit of the presentation of SPL over Strouhal number (Fig. 10, right) is that all peaks occur approximately at the same position. The sound power of the profiles HOM^* and TS^* are in the same range while the profile REF leads to a clearly lower flow noise. The non-weighted sound power level of the reference REF is 73.5 dB and thus 8.5 dB lower than for profile TS^* ($SPL = 82dB$) and 11 dB lower than for profile HOM^* ($SPL = 84,5dB$).

The results show that the flow noise clearly increases for a inhomogeneous flow in the silencer due to local high velocity areas. This must be considered in the design stage, since flow noise should be at least 5 dB lower than the target sound power lever downstream the fan.

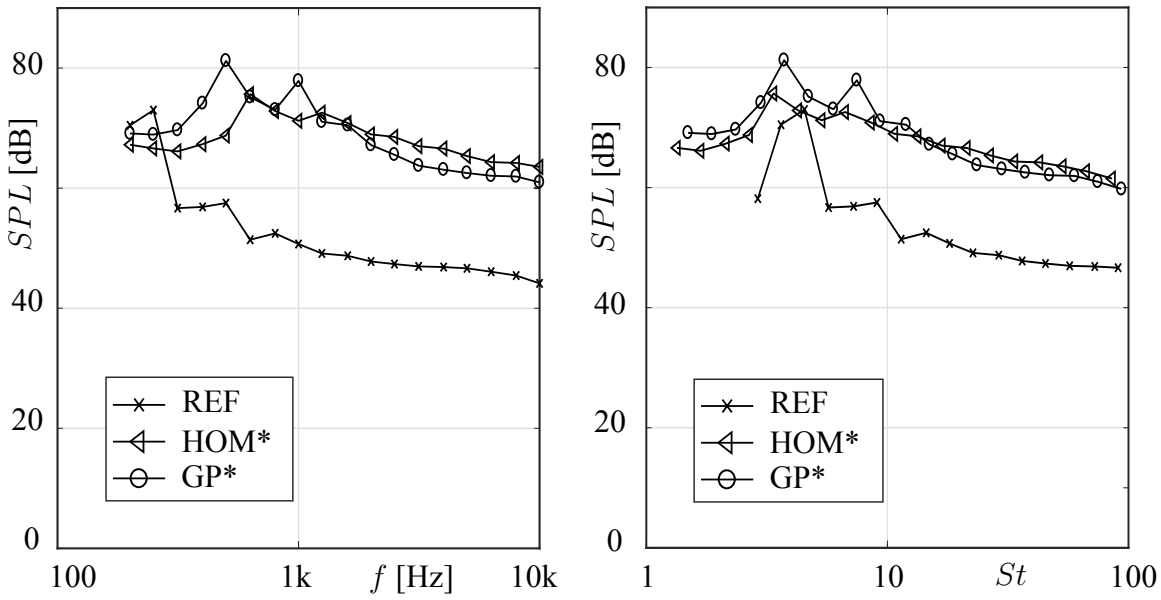

Figure 10: Sound power level SPL for the channel velocity c of $10\,m/s$

CONCLUSION

A non-uniform inflow profile to the silencer unit can considerably increase the areodynamic losses. The loss coefficients are up to 169 % higher than the reference value. The investigation shows that in particular the swirling inflow profiles are disadvantageous. Therefore the fan upstream the silencer unit should have outlet guide vanes to remove the circumferential velocity component. On the one hand, the increased losses can be lead back to the shape of the inflow profile and on the other hand to the adverse pressure gradient in the diffuser and duct transition. The velocity profile between the splitters of the silencer shows local high and low velocity areas due to the latter reasons. The high velocity areas can lead to a considerable generation of flow noise. The noise generation is studied for three different velocity profiles in the silencer with an area averaged velocity of 20 m/s. The non-unform profiles lead to a noise emission which is up to 11dB higher than the noise of the uniform silencer flow profile.

ACKNOWLEDGEMENTS

The author gratefully acknowledges the funding by the German Federal Ministery of Economics (BMWi) in scope of a ZIM project.

REFERENCES

[1] O. Kårekull, G. Efraimsson, and M. Åbom. *Prediction model of flow duct constriction noise*. Applied Acoustics, 82:45–52, **2014**.

[2] H. Fuchs. *Schalldämpfer in Strömungskanälen*. In *Schallabsorber und Schalldämpfer*, pages 497–575. Springer-Verlag, **2010**.

[3] T. Carolus. *Ventilatoren: Aerodynamischer Entwurf, Schallvorhersage, Konstruktion*. Springer-Verlag, **2012**.

[4] *DIN EN ISO 7235:2010-01, Acoustics-Laboratory measurement procedures for ducted silencers and air-terminal units-Insertion loss, flow noise and total pressure loss*. Standard.

[5] J. Walter and M. Gabi. *Investigation of the performance of a fan-diffuser-silencer configuration for thermal power station application*. In *Proceedings of the ISAIF 13*, **2017**.

[6] W. Frommhold. *Absorptionsschalldämpfer*. Technischer Lärmschutz, pages 249–280, **2006**.

[7] F. P. Mechel. *Schallabsorber, Bd 1-3*. S. HirzelVerlag, Stuttgart, **1989**.

[8] G. Sovran and E. Klomp. *Experimentally determined optimum geometries for rectilinear diffusers with rectangular, conical or annular cross-section*. Fluid dynamics of internal flow, pages 271–319, **1967**.

[9] J. Walter, D. Wurz, and M. Gabi. *Investigation of the Performance of Short Diffusers Configurations for Different Inflow Profiles*. Euroturbo 12 Stockholm.

[10] I. Idelchik and E. Fried. *Handbook of hydraulic resistance*. Hemisphere Publishing, **1986**.

[11] U. Ackermann. *Messungen an Schalldämpfern in Kanälen*. Bauphysik, 13(3):77–84, **1991**.

[12] P. Nelson and C. Morfey. *Aerodynamic sound production in low speed flow ducts*. Journal of Sound and Vibration, 79(2):263–289, **1981**.

[13] D. Oldham and A. Ukpoho. *A pressure-based technique for predicting regenerated noise levels in ventilation systems*. Journal of Sound and Vibration, 140(2):259–272, **1990**.

[14] O. Kårekull, G. Efraimsson, and M. Åbom. *Revisiting the Nelson–Morfey scaling law for flow noise from duct constrictions*. Journal of Sound and Vibration, 357:233–244, **2015**.